Human Molecular Genetics, 2003, Vol. 12, No. 3 **329–339**
DOI: 10.1093/hmg/ddg021

An intragenic suppressor in the cytochrome c oxidase I gene of mouse mitochondrial DNA

Rebeca Acín-Pérez, María Pilar Bayona-Bafaluy†, Marta Bueno, Claudia Machicado, Patricio Fernández-Silva, Acisclo Pérez-Martos, Julio Montoya, M.J. López-Pérez, Javier Sancho and José Antonio Enríquez*

Departamento de Bioquímica y Biología Molecular y Celular, Universidad de Zaragoza, Miguel Servet 177, 50013 Zaragoza, Spain

Received October 10, 2002; Revised and Accepted November 13, 2002

We report here the identification of a cell line containing single and double missense mutations in cytochrome c oxidase (COX) subunit I gene of mouse mitochondrial DNA. When present in homoplasmy, the single mutant displays a normal complex IV assembly but a significantly reduced COX activity, while the double mutant almost completely compensates the functional defect of the first mutation. We discuss the potential structural consequences of those mutations based on the modeled structure of mouse complex IV. Based on genetic, biochemical and molecular analyses of cultured mouse cells we infer that: (i) deleterious mutations can arise and become predominant; (ii) cultured cells can maintain several mtDNA haplotypes at stable frequencies; (iii) the respiratory chain has little spare COX capacity; and (iv) the size of a cavity in the vicinity of Val421 in CO I of animal COX may affect the function of the enzyme.

INTRODUCTION

The terminal enzyme of the mitochondrial respiratory chain, cytochrome c oxidase (COX or complex IV), catalyzes the transfer of electrons from reduced cytochrome c to molecular oxygen. The catalytic core of this multimeric complex comprises two subunits (CO I and CO II), and is stabilized by a third subunit (CO III), all of them encoded by the mitochondrial DNA (mtDNA). CO I, II and III are very similar to their homologous proteins in prokaryotes. Ten additional subunits, encoded by the nucleus, are also required in mammals to form fully assembled complex IV (1).

Some diseases in humans are caused by COX deficiency due to mutations in mtDNA-encoded subunits (2). Specifically, six alterations in CO III, four in CO II and three in CO I have been reported (MITOMAP; www.mitomap.org). The investigation in cell culture of a loss of function CO III mutant has allowed it to be confirmed that this subunit does not play a direct role in energy conversion and that it is probably involved in assembly and/or stabilization of complex IV (3). Moreover, missense mutants in CO I, isolated from patients with sideroblastic anemia (Met273Thr and Ile280Thr), are associated with a reduced COX activity and/or stability (4).

To date, human patients have been the only available source for animal mtDNA-encoded complex IV mutants (3,4) and, to our knowledge, such mutants have not been reported in any other animal species, including cultured cell lines (for review see 5). Although mammalian mitochondria cannot be transformed, the mtDNA content of a given cell can be modified, or even fully replaced, by mitochondrial transfer from one cell to another (6). Moreover, this methodology has been recently extended to embryonic stem cells and to zygotes in a way that makes possible to generate trans-mitochondrial mice using cultured cells as a source of the organelles (7–9). However, human mitochondria cannot be successfully transferred to a mouse nuclear background because of an interspecific barrier (10). Therefore, no animal models for COX deficiencies can be generated because of the lack of a source of mutants. Given this situation, the isolation of mouse cells harboring mtDNA mutations would be of special interest since, in addition to the information that cell culture models can provide, they are the only source available for the establishment of mtDNA-transgenic mice. These animals would be an invaluable tool that would provide the model systems required for the better understanding of the assembly, function and physiology of the respiratory complexes. In addition, they would be the only way to determine how a specific pathogenic mutant mtDNA is transmitted and distributed in tissues, resulting in mitochondrial diseases with variable clinical phenotypes, and they would allow the screening of therapeutic drugs and testing gene therapies.

We present here the identification of a mouse cell line harboring, in heteroplasmic form (more than one mtDNA

*To whom correspondence should be addressed. Tel: +34 976761646; Fax: +34 976761612; Email: enriquez@posta.unizar.es
†Present address: Department of Neurology, University of Miami School of Medicine, 1501 NW 9th Avenue Miami, FL 33136, USA.

haplotype present in the same cytoplasm), a single and a double missense mutation in the CO I gene. In our study, the two types of mtDNA have been segregated in different cell lines and their effects have been characterized. Thus, the single missense mutant has a significantly impaired COX activity, with a normal level of assembled complex IV. Very interestingly, the second-site mutant (double mutant) appears to largely compensate for the negative effects of the first mutation. In addition, a structural model has been developed aimed at predicting the molecular consequences of each mutation and at explaining, on structural grounds, the functional effects of the single and double mutants.

RESULTS

Background mutations within the L929 mtDNA

During the course of our investigations aimed at developing a methodology to systematically generate mtDNA mutants in mouse cells, we have sequenced the mtDNA of the L929 mouse cell line. L929 cell line (ATCC CCL-1) is a derivative clone of strain L generated from normal subcutaneous aerolar and adipose tissue of a 100 day-old C3H/An male mouse (11). The mtDNA from L cells was the first mouse mtDNA to be sequenced (12) and is now considered as the mouse mtDNA reference sequence. The number of differences between the L929 mtDNA sequence that we have obtained and the mouse reference sequence was higher than expected. The analysis of the L929 mtDNA sequence and its comparison with the mouse reference and other published sequences (authors unpublished results) showed that three mutations were fixed at relevant frequencies during long-term culture of this cell line and these are the focus of the report.

Two of the mutations identified in L929 lie within the CO I gene [C6063A and T6589C; numbers according to (12)] and a third is an insertion of a C in a stretch of 6Cs located between positions 13887 and 13892 [position 13879 and 13884 in (12)], within the NADH dehydrogenase subunit 6 (ND6) coding sequence. The C6063A transversion in CO I is a missense mutation that changes Leu 246 to Ile. Similarly, the T6589C transition promotes a change from Val 421 to Ala. Sequence chromatograms and RFLP analysis revealed that, of the two CO I mutations, one (T6589C) was present in homoplasmic form (Figs 1A and 2A) while the other (C6063A) was present in 82% of mtDNA molecules (Figs 1B and 2A). On the other hand, the 13887 C insertion in ND 6 was present in 52% of the mtDNA molecules (Figs 1C and 2B). This mutation produces a frameshift starting from the 63rd amino acid, and creates a stop codon 51–53 base pairs downstream of the C stretch, resulting in a 79 amino acid-long truncated polypeptide, instead of the usual 172 amino acid ND6 protein, and it is known to be pathogenic when present in homoplasmy (13).

In summary, the easiest way to explain the presence and frequencies of these mutations is to assume that the L929 culture contains three abundant mtDNA haplotypes (Fig. 2C): the COI^{T6589C}(mtDNA haplotype A, 18%), the COI^{T6589C}/COI^{C6063A} (mtDNA haplotype B, 30%) and the COI^{T6589C}/COI^{C6063A}/$ND6^{13879C}$ (mtDNA haplotype C, 52%).

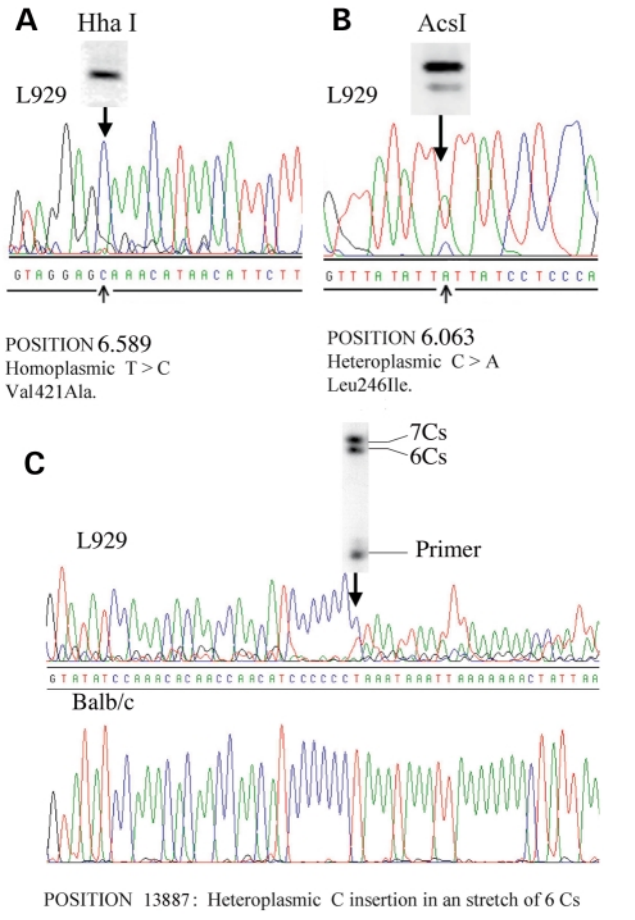

Figure 1. Chromatograms showing the identification of the two missense mutations (**A** and **B**) in the subunit I of the cytochrome c oxidase gene, CO I, and the C insertion (**C**) in the subunit 6 of the NADH dehydrogenase gene, ND6, detected after sequencing the mouse L929 cell line mtDNA. The insets in A and B show the RFLP analysis with the indicated restriction endonuclease that reveals the homoplasmy (A) or the level of heteroplasmy (B) of the CO I missense mutations. The inset in C corresponds to an allele specific termination of primer extension assay to reveal the level of heteroplasmy of the C insertion in the ND6 gene.

Isolation of cells homoplasmic for each CO I mtDNA haplotype

To evaluate the potential phenotypic consequences of the CO I mutations we tried to obtain cell clones pure (homoplasmic) for each genotype. Initially, 34 L929 single cell subclones were generated and the proportion of the heteroplasmic mutation C6063A was first monitored by RFLP analysis to estimate if the single CO I mutant (haplotype A) is located in different cells than the double CO I mutant (haplotypes B and C). The majority of the subclones, 29, were heteroplasmic for the different mtDNA haplotypes with only five being apparently devoid of the A mtDNA and none free of the B/C mtDNA (Fig. 3A). The fact that most of the clones generated out of single cells were still heteroplasmic confirms that the various mtDNA haplotypes co-exist within the same cytoplasm.

In an attempt to force the segregation of the different haplotypes present in L929, cells were partially depleted of mtDNA by treatment with ethidium bromide (EthBr) and then

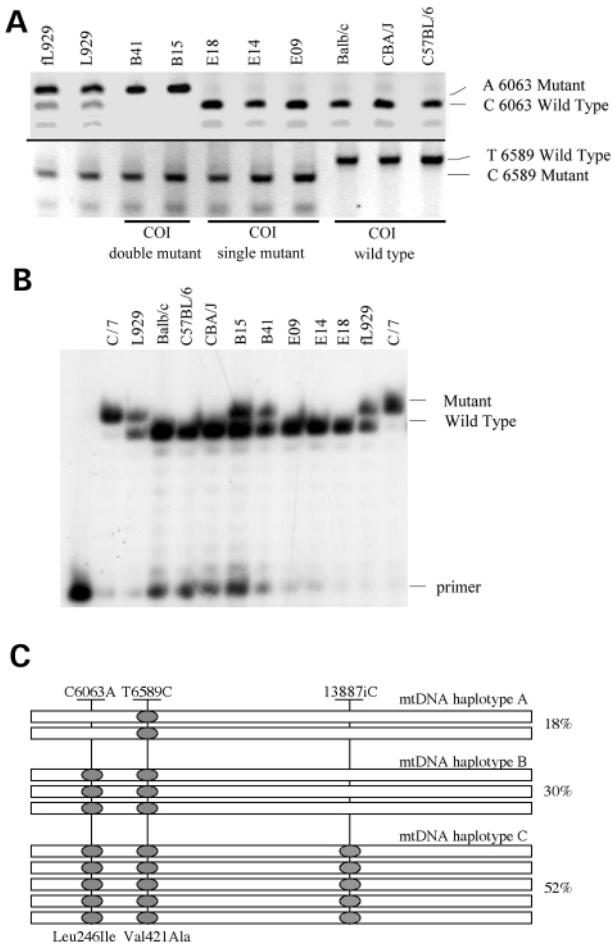

Figure 2. Characterization of the mtDNA genotype of the different cell clones included in the functional study. (**A**, upper panel) RFLP analysis performed with AcsI to show the presence of a C (wild-type) or an A (mutant) at position 6063 within the CO I gene in L929, mice-derived transmitochondrial cells and L929-derived cell clones. (**A**, lower panel) RFLP analysis performed with Hha I to show the presence in homoplasmic form of a T (wild-type) or a C (L929 derived cell clones) at position 6589 of the mouse mtDNA within the CO I gene. (**B**) Allele-specific termination of primer extension to reveal the number of Cs (six or seven) present in each cell line at position 13887 of the mouse mtDNA within the ND6 gene and their proportion [position 13879 in (12)]. (**C**) Diagram representing the three haplotypes of mtDNA detected in the L929 cell line and its relative proportion.

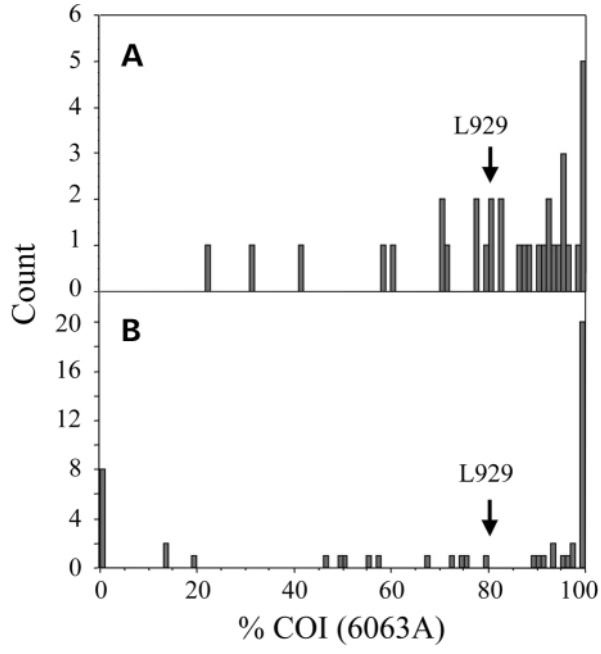

Figure 3. Single cell sub-cloning experiments, without (**A**) or after EthBr treatment of the indicated cell clones (**B**), to segregate in different cells the single CO I mutant (mtDNA haplotype A) from the double CO I mutant (mtDNA haplotypes B/C). The arrows indicate the original level of heteroplasmy in the indicated cell clone.

allowed to recover by removing the drug. Eight of the clones obtained from single cells in this second round of cloning were homoplasmic for the A-haplotype mtDNA and therefore harbored the Val421Ala mutation alone; three of them (E09, E14 and E18) were selected for further analysis (Fig. 2A and B). Twenty additional clones were homoplasmic for the CO I double mutant mtDNA (Fig. 3B), although all these included some genomes with ND6 mutant mtDNA, i.e. haplotype C as well as haplotype B mtDNAs. Repeated rounds of sub-cloning using the same strategy failed to produce cell lines pure for the haplotype-B mtDNA (not shown).

Fortunately, the ND6 ^{13887}C insertion does not influence respiration capacity below 80% of total mtDNAs (Fig. 4A). Moreover, COX activity was not influenced by the presence of the ND6 ^{13887}C insertion at any proportion, even close to 100% mutant (Fig. 4B). Therefore, it was legitimate to investigate the effects of the CO I mutations on the activity of complex IV using cell clones with mixed B/C mtDNA haplotypes. For that purpose we selected two clones, B15 and B41, harboring 72 and 77% of B mtDNA, respectively, the remaining being C-haplotype mtDNA.

In addition, since the wild-type mtDNA haplotype for the CO I gene was absent in the L929 culture, it was obtained by transferring mitochondria from platelets of three different mouse strains (Balb/cJ, C57BL/6J and CBA/J) to an L929 derivative mtDNA-less cell line generated in our laboratory (ρ^{o}L929^{neo}). Thus, three cell lines carrying the wild-type mtDNA (control), three carrying the A-type mtDNA (single CO I mutant) and two carrying B/C mtDNAs (double CO I mutant) were chosen for detailed biochemical and molecular analysis (Fig. 2). As an additional control, mitochondria from the original cell line L929 were also transferred to the ρ^{o}L929^{neo} nuclear background and the resulting transmitochondrial cybrid (fL929) analyzed in parallel with the other cell lines.

COX activity is reduced in the homoplasmic single CO I mutant and recovers in the double mutant

Polarographyc measurements of complex IV activity in digitonin-permeabilized cells (Fig. 5A) revealed that cells homoplasmic for haplotype A (single CO I mutant) have a reduced COX activity (35% of control values; $P < 0.0001$ ANOVA Fisher's PLSD *post-hoc* test). The double CO I mutant cells also showed lower COX activity than control cells (62% of control values; $P < 0.0001$); nevertheless, it was significantly higher than that of the single mutant cells ($P = 0.0011$).

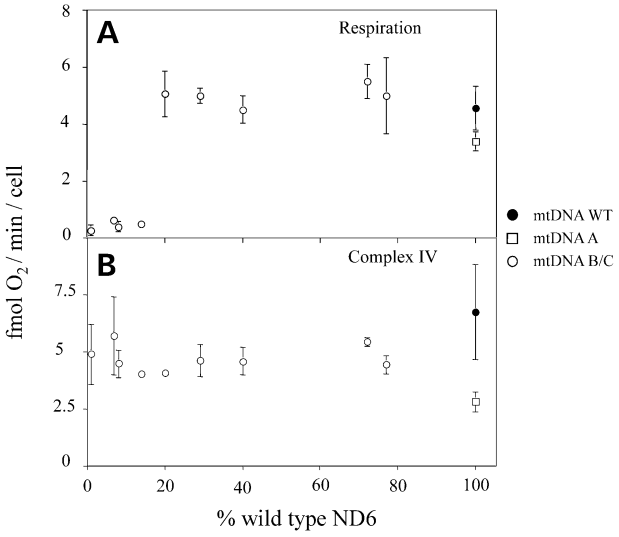

Figure 4. Phenotypic consequences of the C insertion in the ND6 gene on overall respiration (upper panel) and on complex IV activity (lower panel) measured by polarography. Each point of the mtDNA B/C carriers corresponds to the average of a minimum of three measurements of the activity of single cell clones with the indicated proportion of wild type (6C) ND6 mtDNA. Each point of the A or wild-type mtDNA carriers corresponds to the average of the three cell clones included in this study (see Fig. 2) and measured each at least three times. All values are given as mean ± standard deviation of the mean.

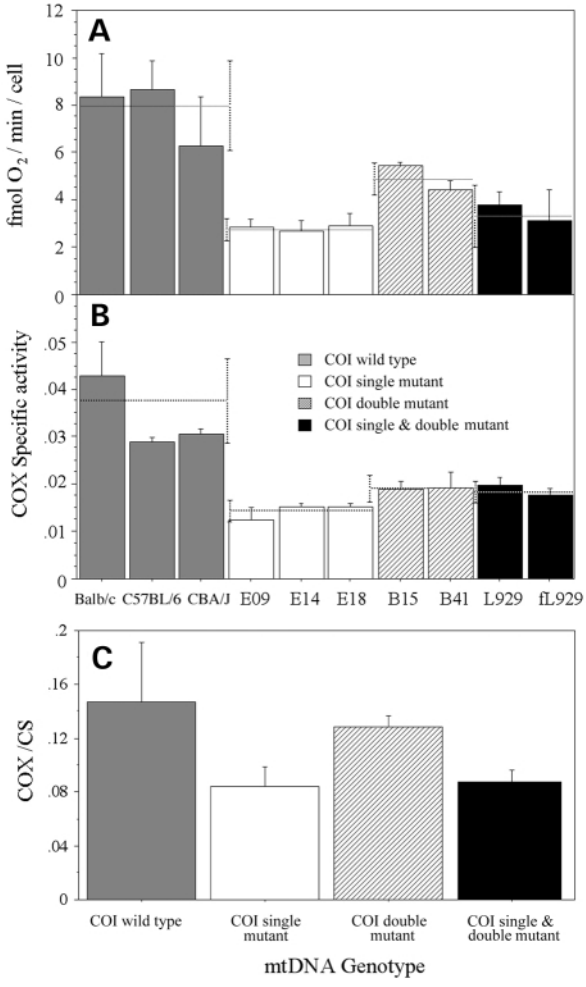

Figure 5. Effect of the CO I genotype on complex IV activity (COX). Data were obtained by (**A**) polarography or (**B** and **C**) spectrophotometry and expressed as (B) specific activity or (C) normalized by the activity of the mitochondrial matrix enzyme citrate synthase (CS). Dotted lines in (A) and (B) represent the average value ± standard deviation of the cell clones belonging to the indicated mtDNA haplotype. All values are given as mean ± SD of the mean. Differences between mtDNA haplotypes tested by ANOVA and the *post-hoc* Fisher PLSD test were always significant with a $P < 0.05$ regardless of the type of analysis or the way of normalization.

Moreover, the TMPD-dependent respiration of the heteroplasmic cell lines L929 and fL929 was intermediate between the homoplasmic single and double mutant cell lines (Fig. 5A).

To confirm that COX activity was different between cell lines with one or two mutations in homoplasmic form, and between mutants and controls, direct measurement of COX activity was also performed by spectrophotometry. As shown in Fig. 5B and C, both COX-specific activity and the COX/CS ratio were lower in the single mutant (37% of control, $P < 0.0001$, and 57% of control, $P < 0.0001$, respectively) than in the double mutant cell lines (50% of control, $P < 0.0001$, and 86% of control, $P = 0.152$, respectively). Again, the heteroplasmic cell lines gave intermediate figures (Fig. 5B and C).

Different oxygen consumption between the homoplasmic single and double mutant cell lines

To investigate if the observed differences in COX activity had consequences for respiration, maximum oxygen consumption capacity was estimated in intact exponentially growing cells (Fig. 6, upper panel). All the cell lines showed a good but characteristic rate of oxygen consumption, from 3.7 to 8.9 fmol/cell/min. However, those cell lines that carried only the T6589C mutation showed a consistently lower rate of oxygen consumption (54% of control, $P < 0.001$) than the double mutant cell lines (82% of control, $P = 0.061$). In addition, the differences in oxygen consumption between the mtDNA variants A and B/C, on average ~34%, were significant ($P < 0.0079$).

Growth advantage of cells carrying the suppressor mutation

The results presented above showed that the OXPHOS competence, and more precisely the COX activity, of cells harboring the Val421Ala mutation in CO I is impaired with respect to control cells. Moreover, the second mutation, within the same gene, acts as an intramolecular suppressor mutation. To evaluate if these mutations influenced the fitness of the cells, the OXPHOS-dependent growth capacity of each cell line was tested in a medium where glucose was substituted by galactose (14). All the cell lines investigated grew rapidly in DMEM (4.5 g/l glucose containing medium supplemented with uridine), with a doubling time (DT) varying between 18.8 and 23.7 h. All these cell lines were able to grow at a good rate when the dependence on mitochondrial OXPHOS was forced by growing them in Leivobitz medium containing galactose instead of glucose (Fig. 6, lower panel). Conversely, a L929 mtDNA-less cell line derivative ($\rho^{o}L929^{neo}$) showed quite good growing ability in uridine-supplemented DMEM medium (DT 18.8 h), but it was unable to survive in galactose-containing medium. In agreement

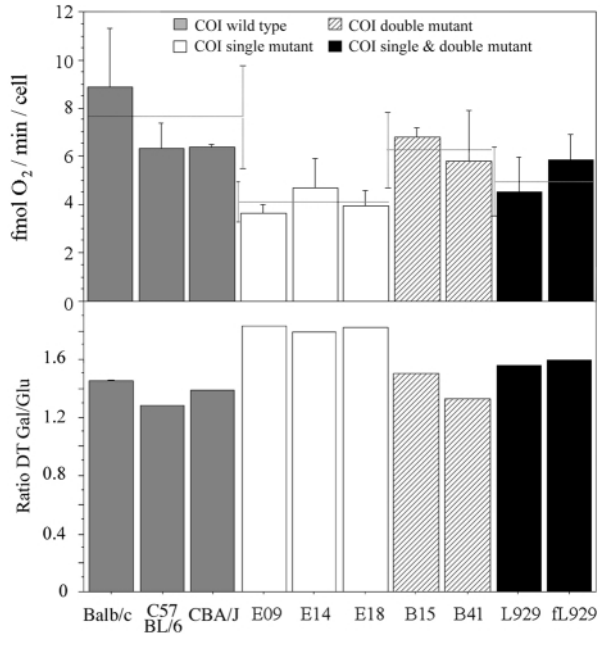

Figure 6. Effect of the CO I genotype on cell phenotype. The overall maximum respiration capacity of the intact uncoupled cells (upper panel) and the cell doubling time (lower panel) in conditions of lower and higher dependence on OXPHOS performance (glucose-enriched medium and galactose medium, respectively) are represented. Differences between mtDNA haplotypes tested by ANOVA and the *post-hoc* Fisher PLSD test were always significant with a $P < 0.05$.

with the biochemical data, about 30% of growth advantage for the double mutant cells and the wild-type cells over the single mutant ones was apparent from the ratio between their doubling time in galactose/glucose (Fig. 6, lower panel).

The Val421Ala change within the CO I protein does not affect complex IV assembly and stability

The reduction in COX associated with mtDNA haplotype A could be due to modifications of either the activity or in the assembly/stability of the complex. To distinguish between these two possibilities we performed Blue-Native gel electrophoresis of the mitochondrial respiratory complexes from representative cell lines of each mtDNA haplotype. Then, to estimate the relative content of COX in the different cell lines, we identified the target complexes with specific antibodies against complexes IV and I. As shown in Figure 7, all tested cell lines maintained a similar relative amount of complex IV/complex I regardless of the mtDNA haplotype they carried (B/C, 1.05; A, 1.16; Balb/cJ, 1; C57BL/6J, 1; CBA/J, 0.9). Therefore, differences in the level of assembled complex IV cannot explain the characteristic COX activity promoted by the different mtDNA haplotypes.

Val421Ala and Leu246Ile changes affect highly conserved amino acids within CO I

The type of residues involved in the two CO I mutations contain aliphatic side-chains, which excludes their direct participation in the electron transport pathway. Nevertheless, these mutations could still induce structural changes that could explain their functional consequences. In order to investigate

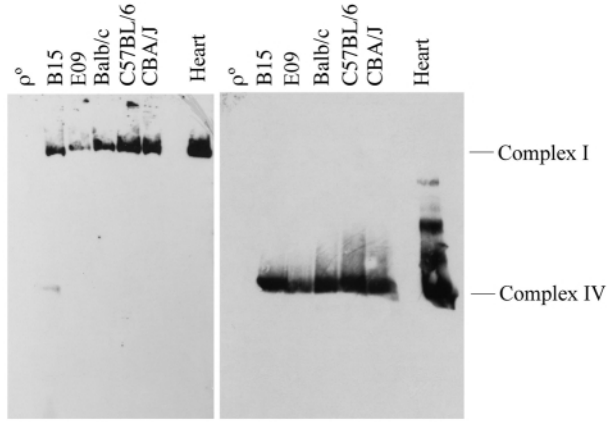

Figure 7. Estimation by Blue-Native electrophoresis and western blot of the relative content of assembled complex I and complex IV in representative cell lines of each mtDNA haplotype. The ratio complex IV/complex I was not significantly different between cell lines.

this possibility, we analyzed the evolutionary relationship of these two residues.

Mutational compensation of protein function can in principle be traced in the form of correlated mutations (15–17). To that end, we have tried to perform a correlation analysis of all the COX sequences available in SWISS-PROT (18). In metazoans (58 sequences) the two positions are totally conserved (as are 30% of all COX residues in this group). When the analysis is extended beyond metazoans, Leu246 is more conserved than Val 421, although in both cases variants are rare (10 and 18 times, respectively, in the 103 sequences analyzed, $P_{246} = 0.10$ and $P_{421} = 0.17$). Thus, the allowed range of substitutions is narrower for Leu246 (Ile, Met and Pro) than for Val421 (Ile, Gln, Ser, Phe, Thr, Met, Tyr and Ala). However, it should be stressed that only two types of Val421 substitution (by Ser or by Ala) were found to occur both in eukaryotes and prokaryotes; the remaining substitutions are confined within a phylogenetic lineage.

In seven of 10 sequences where Leu246 is substituted, a concomitant change at position 421 is observed (usually to Ser but also to Ala; see Fig. 8). Most notably, the Ile/Ala pair of the mouse L929 cell line occurs naturally in the bacterium *Rhodobacter sphaeroides*. Similarly, mutation of Val421 is often accompanied by an additional mutation of Leu246, in seven out 18 occasions. That said, it is modified alone in some eukaryotes, bacteria and archea (Fig. 8). For the 103 sequences analyzed, the probability of both mutations occurring together at random would be $P_{246} \times P_{421} = 0.017$. In other words, 1.7 sequences out of the 103 would be expected to bear mutations in both positions. Instead, seven are found, which suggests that mutations at the two positions are correlated.

The predicted structural consequences of the Val421Ala change within the CO I protein are compensated by the second mutation Leu246Ile

To gain insight into the structural implications of the mutations with diminished COX function we have modeled the mouse enzyme using the bovine one, whose X-ray structure is known (19), as template. The root mean square deviation (RMS) of

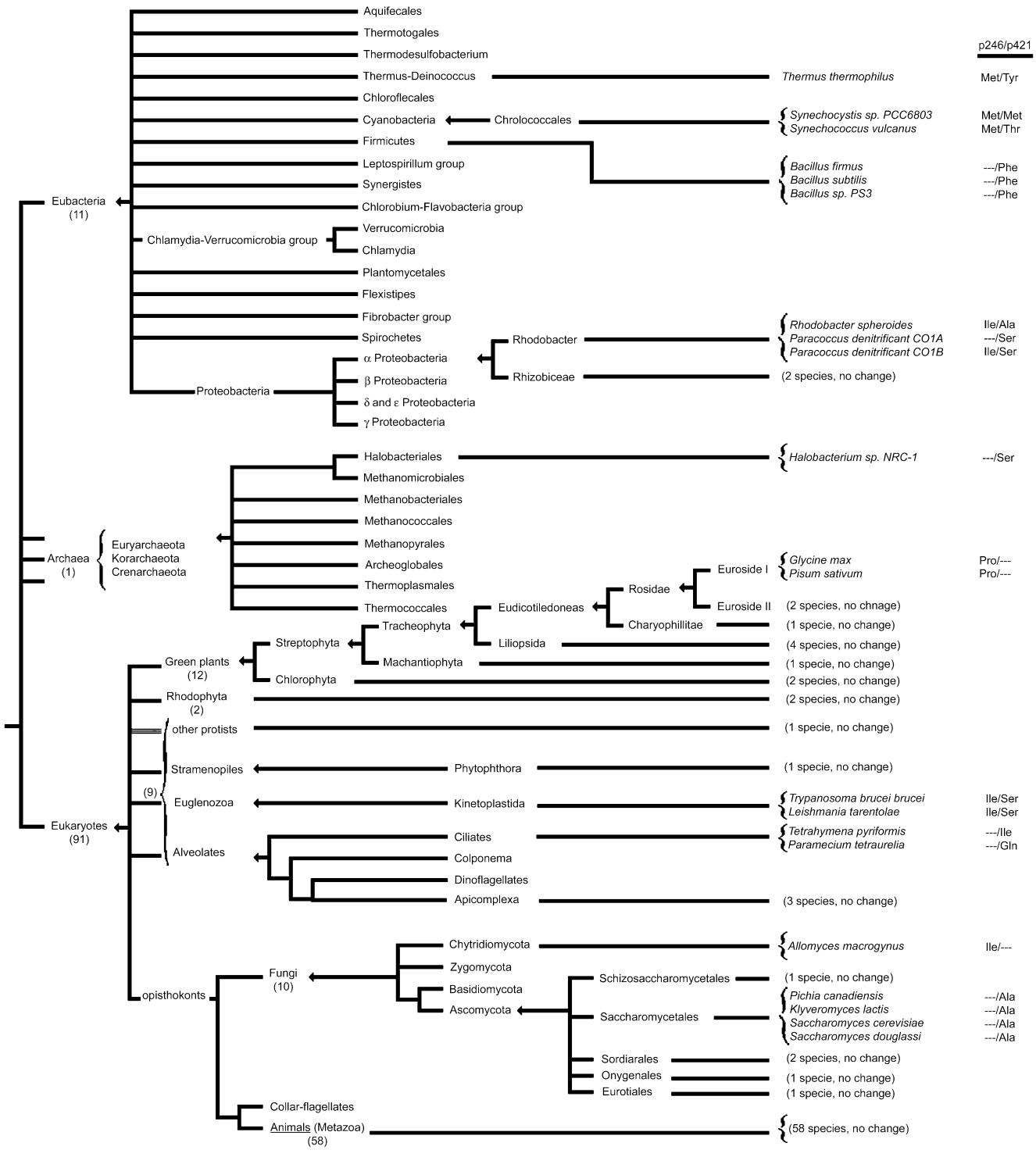

Figure 8. Phylogenetic tree with the 103 CO I sequences available in *SwissProt* database. The occurrence of amino acid substitutions at the homologous 246 and 421 positions (numbering refers to the mouse sequence) is indicated on the right. Numbers in brackets indicate the number of species within a given taxon. 'No change' indicates conservation of both residues as in the wild-type mouse mtDNA.

template and model backbone atoms is of 0.23 Å. The very high homology between the two complexes (93.6% identity) makes the mouse COX model a close approximation to its three-dimensional structure. According to the model, the residues that are different in the mouse and bovine COX complexes are at least 10 Å away from the mutated amino acids.

The first mutation (Val421Ala) is located in helix XII close to Heme a. The wild-type valine is located 5 Å away from the

farnesyl hydroxyl of Heme a and faces a channel running across the interface of helices XI and XII, the so-called channel H (19,20). The second mutation (Leu246Ile) appears in helix VI. The wild-type leucine lays on the surface of the so-called channel D and it is 4 Å away from the nearest Heme (Heme a_3) and 6.5 Å away from Heme a.

We have recently developed a simple procedure that can predict accurately the size and volume of cavities created in proteins by engineered mutations that substitute large residues by smaller ones (21). The method has been tested against 23 cavity mutants of known crystal structure (from three different proteins) and shown to predict very accurately whether the virtual cavity arising from the shortening of the side chain collapses, expands or remains unchanged. The method can only be applied to mutant proteins that are well folded, as is certainly the case with the COX mutants because they remain functional, although with a lower activity. We have applied this method to investigate the effect of the COX mutations on the local protein structure. The first mutation (Val421Ala) enlarges, from 39 to 88 $Å^3$, a pre-existing cavity. This represents a substantial expansion from the theoretical cavity volume of 60 $Å^3$ that should appear upon Val/Ala replacement, in the absence of any local protein rearrangement. The cavity in the Val/Ala mutant is thus two-fold larger than the wild-type cavity and extends along the pore (Fig. 9A). This cavity is very close to the farnesyl hydroxyl of Heme a (20). The hydrogen bonding and cavity patterns at channels D and K are predicted to remain unaffected by the mutation (not shown). The model also predicts that the environment of the two hemes remains unaffected in the mutant (not shown). Thus, the RMS deviation of the heme neighboring groups at ≤ 6 Å in the mutant and wild-type structures is as low as 0.12 Å.

The Leu246Ile mutation represents the introduction of an extra methyl group in the protein core. This group is easily accommodated in a small nearby cavity and does not disrupt the core. In addition, the mutation helps to regularize the dihedral angles of helix VI that appeared slightly distorted near the 246 residue in both wild type and Val421Ala COX. This rearrangement of helix VI is somehow transmitted to helix XI (probably through the intervening helix X, also distorted in this region) because, in the double mutant, the elongated cavity near position 421 shrinks to 59 $Å^3$, almost exactly its predicted value if no additional expansion had occurred concomitant with the Val/Ala mutation (Fig. 9B). In addition, with the second mutation the cavity recovers its spherical shape and thus resembles the original wild-type cavity. Recently, an analogous compensating effect of a distant mutation on the stability and function of the smaller protein lysozyme has been described (22). It is clear that, if our hypothesis that the enlargement and elongation of the cavity associated with the Val421Ala mutation is the cause of the moderate decrease in COX function observed, the Leu246Ile mutation can compensate for the effect of the first one as it restores the cavity shape and size to a closer to wild-type conformation.

DISCUSSION

The results reported here have implications for our understanding of COX function and of mtDNA dynamics in mammalian cells.

Evolution of the mtDNA complement in cultured cells

The norm in mammalian cells is that the sequence of the vast majority of mtDNA molecules should be identical (homoplasmy). This is achieved in animals because, at each new generation, the mtDNA complement derives from clonal expansion of a few copies of maternal mtDNA. In somatic cells however, there is no such a narrow sampling process and heteroplasmy can arise more easily. Despite this, the maintenance and progression of mtDNA variants as well as the level of heteroplasmy is still constrained by the consequences of the mutations for mtDNA and cell fitness. Cells are usually grown in media supplemented with an excess of glucose and other components that reduce their dependence on OXPHOS capacity. In fact, as revealed by biochemical measurements and molecular analysis, the amount and activity of the respiratory complexes in cell culture is significantly lower than in differentiated cells. In this context, the pressures selecting against deleterious mtDNA mutations are significantly relaxed. In this respect, it has been recently shown that different sublines of the original human HeLa cell line have acquired a variety of homoplasmic and heteroplasmic polymorphisms, although their phenotypic relevance has not been defined (23).

The occurrence of three mutations that accumulate to high frequencies in the same cell line (L929 mouse cells) is very intriguing, and we speculate that the T6589C (Val421Ala) mutation appeared first in the cell line, it became homoplasmic in some cells, perhaps by simple genetic drift, and was subsequently sub-cloned (mtDNA haplotype A). In fact, L929 cell clone was established in 1948 by the capillary technique for single cell isolation, being the first cell line derived from the parental L strain (24). After that, an independent event of mutation within the homoplasmic T6589C cell population would originate the C6063A (Leu246Ile) mutation that would become predominant but not homoplasmic (mtDNA haplotype B). The probability of accidentally selecting by random drift two events of mutation, both lying within the same gene, would appear very low. We further speculate that the first mutation could be partially deleterious for the COX and that the second one could totally or partially compensate the defect and therefore its selection was phenotypically driven once it arose. A third mutation event affecting only the mtDNA haplotype B would originate the ND6 frameshift mutation (mtDNA haplotype C). The confirmation that the Val421Ala mutation impairs COX and the Leu246Ile suppresses most of the COX defect supports this interpretation.

Our results corroborate those from human HeLa (23) and other cell models (25–27), indicating that the mtDNA complement in cultured cell lines is not fixed. On the contrary, it mutates and evolves. In addition, we could confirm that all the detected mutations have functional consequences on OXPHOS performance. Moreover, we show that functional deleterious mutations can become predominant, even reaching homoplasmy, and that several mtDNA haplotypes can be observed at stable frequencies in a given cell line. Since the three mtDNA mutations were repeatedly present after single cell sub cloning of the original culture, we can be sure that the three mtDNA haplotypes reside within the same cytoplasm and that very likely they have been or still are present in the same organelle and/or mtDNA nucleoid.

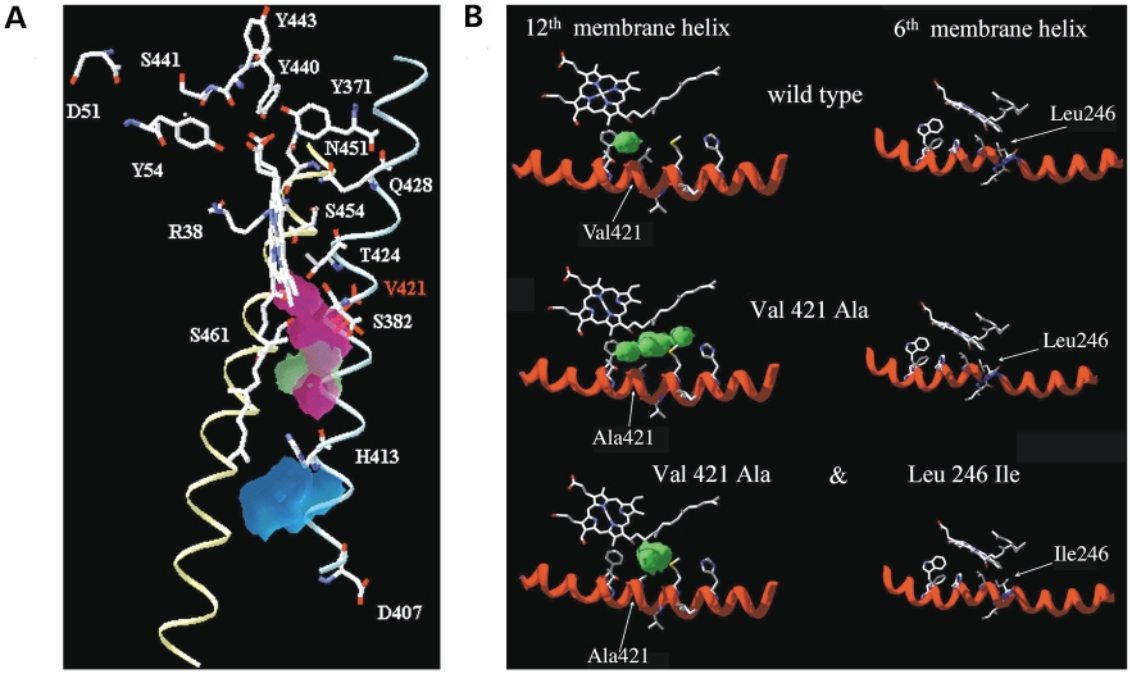

Figure 9. (**A**) Structure of the proposed channel H within the mouse CO I model highlighting the hydrophilic amino acids and the water-containing cavities. The cavity near the Val421 residue (green) is predicted to become larger due to the Val421Ala mutation (mutant cavity in magenta). The cavity near His413 (in blue) is not modified by the mutation. (**B**) Details of the structural models showing the helix XII–heme a and the helix VI–heme a_3 regions of CO I in, from top to bottom, wild-type, Val421Ala (mtDNA haplotype A) and Val421Ala + Leu246Ile (mtDNA haplotypes B/C). The cavities in the structure are shown in green.

How much COX excess is there in animal cells?

A controversial issue regarding the physiological role of the COX activity in mammalian cells is how much the capacity of this enzyme exceeds that which is required to sustain respiration. The question is not trivial and has profound implications for our understanding of mtDNA-linked pathologies in humans. To estimate COX excess, titration experiments with inhibitors of the COX have been performed in isolated mitochondria (28–32), or permeabilized (33,34) or intact cells (35–38). The different approaches produced different conclusions. Using isolated organelles from different sources, a large COX excess of 2–4-fold was estimated depending on the tissue. On the contrary, when using intact cultured cells from different sources, a narrow excess of COX (1.2–1.4 fold) was estimated (35–38). The availability of mutants that promote only a partial decrease in COX activity represents a genetic tool to evaluate the reduction in such activity that can be allowed before affecting respiration. Thus, in our study, the Val421Ala CO I variant was associated with a 43–65% reduction in COX activity, and showed a lower respiration rate than controls. On the contrary, the Leu246Ile/Val421Ala variant was associated with a 25–40% reduction in COX activity and showed normal respiration and growth. Therefore, in agreement with the estimations reported by Villani and Attardi, the excess of COX activity over respiration would be somewhere between 25 and 40% (1.2–1.4-fold) in our cells. Since the technology to transfer whole mitochondria to ES cells or embryos is already available (7–9), our mutants can be used to elucidate the relationship between COX activity, respiration capacity and pathology in the mouse.

Structural hypothesis on the molecular consequences of each mutation

The results presented in this report suggest that the cavity size in the surroundings of Val421 in CO I of animal COX influences the activity of the enzyme. The possible role of such a cavity remains to be clarified. It participates in a putative hydrophilic network inside one of the three pores (pore C) that has been described after the determination of the structure of a bacterial (39) and bovine (19,40) COX. On one side, a regulatory role was attributed to this hydrophilic network (41), but on the other it was proposed that it belongs to a true proton-pumping pathway in animal oxidases, the so-called channel H (20).

Then, our structural hypothesis renders support for a functional role of channel H in animal COX, although it does not allow it to be discerned whether this is related to the function as the proton-pumping pathway or as a regulatory hydrophilic network that does not participate in proton translocation. The definitive answer to this and other alternatives should wait for the generation and isolation of additional mtDNA mutants in animal cells.

The starting point for the generation of an animal model for mtDNA-linked COX deficiency

In conclusion, the more relevant contribution of the research presented in this report is the description and characterization for the first time of a missense mutation in the mtDNA that promotes a significant reduction in COX activity to a level that could become pathological in differentiated cells. Since the

development of methodological approaches for the transference of functional mitochondria from cell lines to embryos, only one true model for mtDNA-linked diseases has been generated (9). This is mainly due to the lack of a variety of characterized mutants in mouse mtDNA. Therefore, the discovery presented in this report opens the possibility of transfering mitochondria from the mutant cells to ES cells or to zygotes in order to generate a mouse with partial COX deficiency. Since the mutation does not abolish completely the activity of the electron transport chain, such a model could be used to determine the tissues or cell types as well the metabolic processes more sensitive to a decrease in the COX capacity and, ultimately, to evaluate therapeutic approaches for mtDNA linked diseases. The behavior of different mitochondrial genotypes in the whole organism may also provide new insights into the segregation of mtDNA.

MATERIALS AND METHODS

Cell lines and media

L929 mouse cells were grown in DMEM (BioWhittaker) supplemented with 5% FBS (fetal bovine serum, GibcoBRL). mtDNA-less mouse cells (ρ^oL929) were generated by long-term growth of the L929 mouse cell line in the presence of high concentrations of EthBr as previously described (42). The ρ^oL929^{neo} cell line is a geneticin-resistant derivative of the ρ^oL929 cell line, obtained by transfection with the neocassette-containing plasmid pcDNA3.1 (Invitrogen), and it was grown in DMEM supplemented with 5% FBS, 50 μg of uridine per ml and 1 mM pyruvate (ρ^o medium), in the presence of 250 μg/ml of geneticin (G418, Sigma). The selective Leivobitz (GibcoBRL) medium supplemented with 5% FBS was used to test OXPHOS growth dependence. This medium contains a low concentration of galactose instead of glucose.

Transfer of mitochondria into ρ^oL929^{neo} cell lines

ρ^oL929^{neo} cell transformation by cytoplast fusion was carried out as previously described (43). Transmitochondrial cell lines were isolated by growing the cell population in DMEM supplemented with 5% dialyzed fetal bovine serum and 500 μg/ml of geneticin (G418). The transference of mitochondria from platelets to ρ^oL929^{neo} was performed as previously described (44).

Oxygen consumption measurements

O_2 consumption determinations in intact cells or in digitonine-permeabilized cells were carried out in an oxigraph with a Clark electrode (Hansatech) as previously described with small modifications (38,45). For determination of the maximum respiration capacity, exponentially growing cells were collected by trypsinization and centrifugation, and resuspended at 6.5×10^6 cells per ml in 0.75 ml of DMEM containing glucose (4.5 g/l), supplemented with 5% FBS, equilibrated at 37°C. Each sample was transferred into a 1.5 ml water-jacketed chamber containing a small magnetic bar, and connected to a circulating water bath at 37°C and a Clark-type oxygen electrode, and recording of oxygen consumption was carried out for 150 s. Then, 2,4-dinitrophenol (DNP, Sigma) to 25–30 μM was added to uncouple the mitochondria in intact cells and oxygen consumption was monitored for 150 additional seconds to determine the maximum O_2 consumption of each cell line.

For determination of the complex IV-dependent respiration cell samples were resuspended at 5.0×10^6 cells per ml in 1 ml of a buffer containing 20 mM HEPES pH 7.1, 250 mM sucrose, 10 mM $MgCl_2$, 1 mM ADP and 2 mM Pi. Then, the oxygen consumption was measured as described above but after addition of: digitonine (8 μg per million cells) to permeabilize the cell membrane, rotenone (Sigma) (100 nM) to inhibit complex I-dependent respiration; antimycin A (Sigma) (20 nM) to inhibit complex II + III dependent respiration; and TMPD (*N*,*N*,*N*′,*N*′-tetramethyl-*p*-phenylenediamine; Sigma; 0.1–2.0 mM) as a direct electron donor to complex IV.

DNA analysis and mtDNA sequencing

Total DNA was isolated from cells by digestion with proteinase K in buffer TE (Tris 10 mM, EDTA 1 mM, pH 7.5), containing 0.5% SDS and ribonuclease A, purified by extraction with phenol–chloroform–isoamyl alcohol and precipitated with ethanol. Overlapping segments of 1000–1500 bp covering the entire mtDNA were amplified by PCR, with the appropriate oligodeoxynucleotides. The PCR products were purified using the rapid PCR purification system of Gibco BRL, and the purified double stranded fragments were directly sequenced by the chain termination method, using nested primers.

Quantification of the CO I 6063 and 6589 mutations was achieved by RFLP analysis. Thus, a 177 bp fragment containing the 6063 site was amplified by polymerase chain reaction with the following primers: (1) forward, GCATCTGTTCTGATTCTTTGGGCACCCAGAAGTTTAaATT (positions 6023–6062, forward primer carrying a mismatch indicated by the lower case a); (2) reverse, GTGGTGGGCTCATACAATAAAGC (positions 6200–6178).

The combination of the PCR-generated mutation together with the wild-type version at the 6063 site generates a recognition site for Acs I. Thus, the presence of the 6063 mutation disrupts the restriction site.

To analyze the 6589 mutation, a 125 bp fragment was amplified by polymerase chain reaction with the following primers: (1) forward, CATGAGCAAAAGCCCACTTCGCCATCATATTCGTAGGcG (position 6550–6588, forward primer carrying a mismatch indicated by the lower case c); (2) reverse, TGTGGTGTAAGCATCTGGGTAG (position 6653–6674, reverse primer).

The combination of the PCR-generated mutation together with the mutant version at the 6589 site (6589C) creates a recognition site for Hha I. Thus, the presence of the 6589T (wild-type) disrupts the restriction site.

The fragments generated after digestion with the corresponding enzyme were visualized by electrophoresis in a 3% agarose gel containing 0.5 μg/ml EthBr. Quantification of the ND6 C insertion was achieved by allele specific termination of primer extension (13).

Analysis of assembled complex I and IV by Blue native electrophoresis

Estimation of the relative level of complex IV assembly in the control and mutant cell lines was performed by Blue-Native electrophoresis (BN–PAGE) according to Schägger (46). After electrophoresis, the complexes were electroblotted onto nylon filters and sequentially probed with specific antibodies against complex I (anti-NDUSF3, kindly gifted by Dr R. A. Capaldi), and complex IV (anti-CO I, Molecular Probes). The specific complexes were detected by the 'ECL western blotting detection analysis system' from Amersham. The signal obtained with each antibody was quantified on autoradiography films using a laser densitometer and the ratio of complex I to complex IV specific intensities was determined for each cell line.

Modeling of the mouse COX complex

The mouse COX complex (13 subunits) was modeled with *SwissModel* (47) using several structures of the bovine heart COX as templates (PDB codes: 100C, 10CO, 10CR, 10CZ and 200C). Some of the shorter subunits were, however, modeled after the corresponding subunits from other species (PDB codes: 1EHK, 1AR1, 1QLE and 1FFT). The identity between template and target subunit sequences varied from 100% (subunit V) to 63% (subunit VIII). The identity for subunit I was 93.6%. The original model was analyzed with *WHATCHECK* (as implemented in *WHATIF*) (48) and a number of non-satisfactory distances and angles where refined by 500 steps of steepest descents using *CHARMm* (49) as implemented in *InsightII* (MSI Inc). The model was then analyzed with *PROCHECK* (50), which detected no geometrical errors.

Modeling of the Val421Ala and Val421Ala/Leu246Ile COX mutations

The modeling of mutations involving hydrophobic buried residues was done as described (21). All minimizations were carried out using the *CHARMm* force field (49) as implemented in *Insight* II (MSI Inc). A cut-off distance of 11 Å was used for non-bonded interactions (with smoothing from 8 Å). 2000 steps of steepest descents were applied to each structure in an unconstrained path. Minimizations were started from the modeled structures of the mouse wild-type COX after having implemented the appropriate *in silico* mutations. Two mutants were modeled: Val421Ala and Val421Ala/Leu246Ile. Cavity volumes were calculated using the Connolly method with a probe radius of 1.4 Å (51).

Protein sequence alignments

Homologs of the mouse COX sequence were identified with *BLAST* (52) and preliminarily aligned with *CLUSTALW* (53). Incomplete sequences bearing more than 15% gaps or less than 30% identities were discarded and the remaining sequences were realigned. *BioEdit* was used to extract the alignment information.

ACKNOWLEDGEMENTS

We would like to thank Dr R. A. Capaldi for the kind gift of the anti-NDUFS3 antibody, and to Raquel Moreno-Loshuertos, Erika Fernández-Vizarra, Jesús Tejero and Santiago Morales for their technical assistance. Our research was supported by the Spanish Ministry of Education PM-99-0082 grant to J.A.E., by the Spanish Ministry of Science and Technology BMC 2001-252 and DGA P120/2001 grants to J.S., by the Ramón y Cajal 2001 grant to P.F.S and by the Ramón Areces 1997 grant to M.J.L.P. R.A.-P. and M.B. are recipients of the Spanish F.P.U. fellowships, and C.M. of the Spanish AECI fellowship.

REFERENCES

1. Abramson, J., Svensson-Ek, M., Byrne, B. and Iwata, S. (2001) Structure of cytochrome c oxidase: a comparison of the bacterial and mitochondrial enzymes. *Biochim. Biophys. Acta*, **1544**, 1–9.
2. Shoubridge, E.A. (2001) Cytochrome c oxidase deficiency. *Am. J. Med. Genet.*, **106**, 46–52.
3. Tiranti, V., Corona, P., Greco, M., Taanman, J.W., Carrara, F., Lamantea, E., Nijtmans, L., Uziel, G. and Zeviani, M. (2000) A novel frameshift mutation of the mtDNA COIII gene leads to impaired assembly of cytochrome c oxidase in a patient affected by Leigh-like syndrome. *Hum. Mol. Genet.*, **9**, 2733–2742.
4. Broker, S., Meunier, B., Rich, P., Gattermann, N. and Hofhaus, G. (1998) MtDNA mutations associated with sideroblastic anaemia cause a defect of mitochondrial cytochrome c oxidase. *Eur. J. Biochem.*, **258**, 132–138.
5. Bayona-Bafaluy, P., Fernández-Silva, P. and Enriquez, J.A. (2003) The thankless task of playing genetics with mammalian mitochondrial DNA—a 30 year review. *Mitochondrion*, **2**, 3–25.
6. King, M.P. and Attardi, G. (1989) Human cells lacking mtDNA: repopulation with exogenous mitochondria by complementation. *Science*, **246**, 500–503.
7. Sligh, J.E., Levy, S.E., Waymire, K.G., Allard, P., Dillehay, D.L., Nusinowitz, S., Heckenlively, J.R., MacGregor, G.R. and Wallace, D.C. (2000) Maternal germ-line transmission of mutant mtDNAs from embryonic stem cell-derived chimeric mice. *Proc. Natl Acad. Sci. USA*, **97**, 14461–14466.
8. Marchington, D.R., Barlow, D. and Poulton, J. (1999) Transmitochondrial mice carrying resistance to chloramphenicol on mitochondrial DNA: developing the first mouse model of mitochondrial DNA disease. *Nat. Med.*, **5**, 957–960.
9. Inoue, K., Nakada, K., Ogura, A., Isobe, K., Goto, Y., Nonaka, I. and Hayashi, J.I. (2000) Generation of mice with mitochondrial dysfunction by introducing mouse mtDNA carrying a deletion into zygotes. *Nat. Genet.*, **26**, 176–181.
10. Kenyon, L. and Moraes, C.T. (1997) Expanding the functional human mitochondrial DNA database by the establishment of primate xenomitochondrial cybrids. *Proc. Natl Acad. Sci. USA*, **94**, 9131–9135.
11. Earle, W.R., Schilling, E.L., Stark, T.H., Straus, N.P., Brown, M.F. and Shelton, E. (1943) Production of malignancy *in vitro*. IV. The mouse fibroblast cultures and changes seen in the living cells. *J. Natl Cancer Inst.*, **4**, 165–212.
12. Bibb, M.J., Van Etten, R.A., Wright, C.T., Walberg, M.W. and Clayton, D.A. (1981) Sequence and gene organization of mouse mitochondrial DNA. *Cell*, **26**, 167–180.
13. Bai, Y. and Attardi, G. (1998) The mtDNA-encoded ND6 subunit of mitochondrial NADH dehydrogenase is essential for the assembly of the membrane arm and the respiratory function of the enzyme. *Embo J.*, **17**, 4848–4858.
14. Chu, E.H., Sun, N.C. and Chang, C.C. (1972) Induction of auxotrophic mutations by treatment of Chinese hamster cells with 5-bromodeoxyuridine and black light. *Proc. Natl Acad. Sci. USA*, **69**, 3459–3463.
15. Vernet, T., Tessier, D.C., Khouri, H.E. and Altschuh, D. (1992) Correlation of co-ordinated amino acid changes at the two-domain interface of cysteine proteases with protein stability. *J. Mol. Biol.*, **224**, 501–509.
16. Singer, M.S., Oliveira, L., Vriend, G. and Shepherd, G.M. (1995) Potential ligand-binding residues in rat olfactory receptors identified by correlated mutation analysis. *Receptors Channels*, **3**, 89–95.

17. Mateu, M.G. and Fersht, A.R. (1999) Mutually compensatory mutations during evolution of the tetramerization domain of tumor suppressor p53 lead to impaired hetero-oligomerization. *Proc. Natl Acad. Sci. USA*, **96**, 3595–3599.
18. Bairoch, A. and Apweiler, R. (2000) The SWISS-PROT protein sequence database and its supplement TrEMBL in 2000. *Nucl. Acids Res.*, **28**, 45–48.
19. Tsukihara, T., Aoyama, H., Yamashita, E., Tomizaki, T., Yamaguchi, H., Shinzawa-Itoh, K., Nakashima, R., Yaono, R. and Yoshikawa, S. (1996) The whole structure of the 13-subunit oxidized cytochrome c oxidase at 2.8 A. *Science*, **272**, 1136–1144.
20. Yoshikawa, S., Shinzawa-Itoh, K., Nakashima, R., Yaono, R., Yamashita, E., Inoue, N., Yao, M., Fei, M.J., Libeu, C.P., Mizushima, T. *et al.* (1998) Redox-coupled crystal structural changes in bovine heart cytochrome c oxidase. *Science*, **280**, 1723–1729.
21. Machicado, C., Bueno, M. and Sancho, J. (2002) Predicting the structure of protein cavities created by mutation. *Protein Engng*, **15**, 669–675.
22. Wray, J.W., Baase, W.A., Lindstrom, J.D., Weaver, L.H., Poteete, A.R. and Matthews, B.W. (1999) Structural analysis of a non-contiguous second-site revertant in T4 lysozyme shows that increasing the rigidity of a protein can enhance its stability. *J. Mol. Biol.*, **292**, 1111–1120.
23. Herrnstadt, C., Preston, G., Andrews, R., Chinnery, P., Lightowlers, R.N., Turnbull, D.M., Kubacka, I. and Howell, N. (2002) A high frequency of mtDNA polymorphisms in HeLa cell sublines. *Mutat. Res.*, **501**, 19–28.
24. Sanford, K.K., Earle, W.R. and Likely, G.d. (1948) The growth *in vitro* of single isolated tissue cells. *J. Natl Cancer Inst.*, **9**, 229–246.
25. Yoneda, M., Chomyn, A., Martinuzzi, A., Hurko, O. and Attardi, G. (1992) Marked replicative advantage of human mtDNA carrying a point mutation that causes the MELAS encephalomyopathy. *Proc. Natl Acad. Sci. USA*, **89**, 11164–11168.
26. Dunbar, D.R., Moonie, P.A., Jacobs, H.T. and Holt, I.J. (1995) Different cellular backgrounds confer a marked advantage to either mutant or wild-type mitochondrial genomes. *Proc. Natl Acad. Sci. USA*, **92**, 6562–6566.
27. Lehtinen, S.K., Hance, N., El Meziane, A., Juhola, M.K., Juhola, K.M., Karhu, R., Spelbrink, J.N., Holt, I.J. and Jacobs, H.T. (2000) Genotypic stability, segregation and selection in heteroplasmic human cell lines containing np 3243 mutant mtDNA. *Genetics*, **154**, 363–380.
28. Letellier, T., Heinrich, R., Malgat, M. and Mazat, J.P. (1994) The kinetic basis of threshold effects observed in mitochondrial diseases: a systemic approach. *Biochem. J.*, **302**, 171–174.
29. Letellier, T., Malgat, M. and Mazat, J.P. (1993) Control of oxidative phosphorylation in rat muscle mitochondria: implications for mitochondrial myopathies. *Biochim. Biophys. Acta*, **1141**, 58–64.
30. Davey, G.P. and Clark, J.B. (1996) Threshold effects and control of oxidative phosphorylation in nonsynaptic rat brain mitochondria. *J. Neurochem.*, **66**, 1617–1624.
31. Davey, G.P., Canevari, L. and Clark, J.B. (1997) Threshold effects in synaptosomal and nonsynaptic mitochondria from hippocampal CA1 and paramedian neocortex brain regions. *J. Neurochem.*, **69**, 2564–2570.
32. Davey, G.P., Peuchen, S. and Clark, J.B. (1998) Energy thresholds in brain mitochondria. Potential involvement in neurodegeneration. *J. Biol. Chem.*, **273**, 12753–12757.
33. Kuznetsov, A.V., Clark, J.F., Winkler, K. and Kunz, W.S. (1996) Increase of flux control of cytochrome c oxidase in copper-deficient mottled brindled mice. *J. Biol. Chem.*, **271**, 283–288.
34. Kuznetsov, A.V., Winkler, K., Kirches, E., Lins, H., Feistner, H. and Kunz, W.S. (1997) Application of inhibitor titrations for the detection of oxidative phosphorylation defects in saponin-skinned muscle fibers of patients with mitochondrial diseases. *Biochim. Biophys. Acta*, **1360**, 142–150.
35. Villani, G. and Attardi, G. (2000) *In vivo* control of respiration by cytochrome c oxidase in human cells. *Free Radic. Biol. Med.*, **29**, 202–210.
36. Kunz, W.S., Kudin, A., Vielhaber, S., Elger, C.E., Attardi, G. and Villani, G. (2000) Flux control of cytochrome c oxidase in human skeletal muscle. *J. Biol. Chem.*, **275**, 27741–27745.
37. Villani, G., Greco, M., Papa, S. and Attardi, G. (1998) Low reserve of cytochrome c oxidase capacity *in vivo* in the respiratory chain of a variety of human cell types. *J. Biol. Chem.*, **273**, 31829–31836.
38. Villani, G. and Attardi, G. (1997) *In vivo* control of respiration by cytochrome c oxidase in wild-type and mitochondrial DNA mutation-carrying human cells. *Proc. Natl Acad. Sci. USA*, **94**, 1166–1171.
39. Iwata, S., Ostermeier, C., Ludwig, B. and Michel, H. (1995) Structure at 2.8 A resolution of cytochrome c oxidase from *Paracoccus denitrificans*. *Nature*, **376**, 660–669.
40. Tsukihara, T., Aoyama, H., Yamashita, E., Tomizaki, T., Yamaguchi, H., Shinzawa-Itoh, K., Nakashima, R., Yaono, R. and Yoshikawa, S. (1995) Structures of metal sites of oxidized bovine heart cytochrome c oxidase at 2.8 A. *Science*, **269**, 1069–1074.
41. Lee, H.M., Das, T.K., Rousseau, D.L., Mills, D., Ferguson-Miller, S. and Gennis, R.B. (2000) Mutations in the putative H-channel in the cytochrome c oxidase from Rhodobacter sphaeroides show that this channel is not important for proton conduction but reveal modulation of the properties of heme a. *Biochemistry*, **39**, 2989–2996.
42. Tiranti, V., Hoertnagel, K., Carrozzo, R., Galimberti, C., Munaro, M., Granatiero, M., Zelante, L., Gasparini, P., Marzella, R., Rocchi, M. *et al.* (1998) Mutations of SURF-1 in Leigh disease associated with cytochrome c oxidase deficiency. *Am. J. Hum. Genet.*, **63**, 1609–1621.
43. King, M.P. and Attardi, G. (1996) Isolation of human cell lines lacking mitochondrial DNA. *Meth. Enzymol.*, **264**, 304–313.
44. Chomyn, A., Lai, S.T., Shakeley, R., Bresolin, N., Scarlato, G. and Attardi, G. (1994) Platelet-mediated transformation of mtDNA-less human cells: analysis of phenotypic variability among clones from normal individuals—and complementation behavior of the tRNALys mutation causing myoclonic epilepsy and ragged red fibers. *Am. J. Hum. Genet.*, **54**, 966–974.
45. Hofhaus, G., Shakeley, R.M. and Attardi, G. (1996) Use of polarography to detect respiration defects in cell cultures. *Meth. Enzymol.*, **264**, 476–483.
46. Schagger, H. (1996) Electrophoretic techniques for isolation and quantification of oxidative phosphorylation complexes from human tissues. *Meth. Enzymol.*, **264**, 555–566.
47. Guex, N. and Peitsch, M.C. (1997) SWISS-MODEL and the Swiss-PdbViewer: an environment for comparative protein modeling. *Electrophoresis*, **18**, 2714–2723.
48. Vriend, G. (1990) WHAT IF: a molecular modeling and drug design program. *J. Mol. Graph.*, **8**, 52–56, 29.
49. Brooks, B., Bruccoleri, R., Olafson, B., States, D., Swaminathan, S. and Karplus, M. (1983) CHARMM: a program for macromolecular energy, minimisation, and dynamics calculations. *J. Comput. Chem.*, **4**, 187–217.
50. Laskowski, R.A., MacArthur, M.W. and Moss, D.S. (1993) PROCHECK: a program to check the stereochemical quality of protein structures. *J. Appl. Crystallogr.*, **26**, 283–291.
51. Connolly, M.L. (1983) Solvent-accessible surfaces of proteins and nucleic acids. *Science*, **221**, 709–713.
52. Altschul, S.F., Gish, W., Miller, W., Myers, E.W. and Lipman, D.J. (1990) Basic local alignment search tool. *J. Mol. Biol.*, **215**, 403–410.
53. Thompson, J.D., Higgins, D.G. and Gibson, T.J. (1994) CLUSTAL W: improving the sensitivity of progressive multiple sequence alignment through sequence weighting, position-specific gap penalties and weight matrix choice. *Nucl. Acids Res.*, **22**, 4673–4680.